MIMO Radar Optimization With Constant-Modulus and Any p-Norm Similarity Constraints

Xin He, *Member, IEEE*,

***Abstract*—MIMO radar plays a key role in autonomous driving, and the similarity waveform constraint is an important constraint for radar waveform design. However, the joint constant-modulus and similarity constraint is a difficult constraint. Only the special case with ∞-norm similarity and constant-modulus constraints is tackled by the semidefinite relaxation (SDR) and the successive quadratic refinement (SQR) methods. In this paper, the joint constant-modulus and any p-norm ($1 \leq p \leq \infty$) similarity constraint is tackled by the proposed relax-and-retract algorithm. In particular, the nonconvex constant-modulus constraint is first relaxed to convex constraint, and then the retract operation is guaranteed to recover a constant-modulus solution within a fixed iteration number. Extensive simulation results show that full range similarity control and constant-modulus constraints are satisfied under different p-norms. For the special case with 1-norm, it is firstly found to be a constant-modulus-inducing norm. For the special case with ∞-norm, the proposed relax-and-retract method has less computational time than the SDR and SQR methods.**

***Index Terms*—MIMO Radar, Constant-Modulus, Unit-Modulus, p-Norm, Similarity Constraint, Relax-and-Retract.**

I. Introduction

Radar waveform design has been attracting much attention lately in autonomous driving [1]. MIMO radar can obtain a higher spatial resolution and a better detection performance compared with a phased-array radar [2]. For practical consideration, two sets of constraints were introduced to the MIMO radar waveform design: similarity constraint and constant-modulus constraint [3]–[5].

In order to control the radar waveform's peak sidelobe level, the 2-norm similarity waveform constraint was introduced in [4]. To restrict the transmit power, the 2-norm similarity constraint and the per-antenna power constraint was proposed in [2]. The Doppler accuracy and 2-norm similarity constraints were proposed in [6], and the semidefinite relaxation (SDR) was used to tackle the problem.

To better utilize the nonlinear power amplifier, the constant-modulus constraint was introduced in [5]. Owing to the difficult of the nonconvex constant-modulus constraint, the similarity constraint in [5] was restricted to be ∞-norm. The ∞-norm similarity and constant-modulus constraints were proposed in the MIMO radar waveform design [7], and the technique is the SDR method. To reduce the computational complexity of the SDR method, the successive quadratic refinement (SQR) method [8] was proposed to tackle the ∞-norm similarity and constant-modulus constraints. Owing to special property of the ∞-norm, the ∞-norm similarity restriction turns out to be a simple phase restriction [5], [7], [8]. With multiple targets, an iterative algorithm was proposed in [9], but the constant-modulus solution is not guaranteed. In order to tackle the ∞-norm similarity and constant-modulus constraints with lower computational complexity, the majorization-minimization (MM) method was applied in [10] and the alternation direction method of multipliers (ADMM) method was proposed in [11], which did not guarantee a constant-modulus solution. Therefore, all existing radar waveform design with constant-modulus constraint and similarity constraint under other p-norms is not available.

In this paper, we propose to solve the MIMO radar waveform design problem with the constant-modulus constraint and similarity constraint associated with any p-norm, where $1 \leq p \leq \infty$. The methodology of the relax-and-retract algorithm is extended from the communication problem [12] to tackle the radar waveform design problem. Extensive simulation results show that full range similarity control and constant-modulus constraints are satisfied under different p-norms. The contributions of the paper are summarized as follows.

- Under constant-modulus constraint, all existing methods are only suitable for ∞-norm similarity constraint, while the proposed method is valid for p-norm with $1 \leq p \leq \infty$.
- Some existing methods are not guaranteed to provide constant-modulus solution, while the proposed method guarantees to provide constant-modulus solution within a fixed iteration number.
- For the special case with 1-norm, it is firstly observed to be a constant-modulus-inducing norm.
- For the special case with ∞-norm, the proposed relax-and-retract method has less computational time than the SDR and SQR methods.

Notations. We use boldface letters to represent vectors and matrices, and the notation $(\cdot)^T$ and $(\cdot)^H$ denote transposition and Hermitian, respectively, $\|\cdot\|_p$ denotes the p-norm of a vector. In addition, $\mathrm{Re}\,(\cdot)$ and $\mathrm{Im}\,(\cdot)$ refer to the real and imaginary part of a complex number, respectively. The notations $\mathrm{vec}\,(\cdot)$ and $\otimes$ stand for the vectorization and Kronecker product, respectively. $\mathbf{I}_L$ is a $L \times L$ identity matrix, $j = \sqrt{-1}$, and $\mathbf{s}(n)$ is the n-th element of the vector $\mathbf{s}$.

II. System Model

The radar system is a collocated MIMO radar system, the transmit antenna number is M_t, the receive antenna number is M_r, and the antennas are arranged into a uniform linear array

Xin He is with the College of Electronics and Information Engineering, Shenzhen University, China. Xin He is also with Hanshan Normal University, Chaozhou, China. Email: hx66hx@gmail.com. ORCID iD: 0000-0002-2248-4742. This work was supported in part by the National Natural Science Foundation of China under Grants 61807018.

with interelement spacing d_t and d_r, respectively. The number of the far-field targets is K_t, the distinct angles are $\{\theta_k\}$, the target reflection coefficients are $\{\beta_k\}$, and the Doppler shifts are $\{\nu_k\}$. The steering vectors are defined as follows [13],

$$\mathbf{v}_t(\theta)=\frac{1}{\sqrt{M_t}}[1, e^{j2\pi d_t \sin(\theta)/\lambda}, \cdots e^{j2\pi(M_t-1)d_t \sin(\theta)/\lambda}]^T, \tag{1}$$

$$\mathbf{v}_r(\theta)=\frac{1}{\sqrt{M_r}}[1, e^{j2\pi d_r \sin(\theta)/\lambda}, \cdots e^{j2\pi(M_r-1)d_r \sin(\theta)/\lambda}]^T, \tag{2}$$

where λ is the carrier wavelength. Therefore, the target response matrix is modeled as

$$\mathbf{V}_1 = \sum_{k=1}^{K_t} \beta_k e^{j2\pi\nu_k} \mathbf{v}_r(\theta_k)\mathbf{v}_t(\theta_k)^T. \tag{3}$$

In the clutter, K_c point scatterers are estimated at angles $\{\theta_{k,c}\}$, with reflection coefficients $\{\beta_{k,c}\}$ and Doppler shifts $\{\nu_{k,c}\}$. Similarly, the clutter response matrix is modelled as

$$\mathbf{V}_2 = \sum_{k=1}^{K_c} \beta_{k,c} e^{j2\pi\nu_{k,c}} \mathbf{v}_r(\theta_{k,c})\mathbf{v}_t(\theta_{k,c})^T. \tag{4}$$

With transmitted waveform $\mathbf{S} = [\mathbf{s}_1, \cdots, \mathbf{s}_L] \in \mathbb{C}^{M_t \times L}$, the received signal at the radar receiver is

$$\mathbf{Y} = \mathbf{V}_1\mathbf{S} + \mathbf{V}_2\mathbf{S} + \mathbf{N}, \tag{5}$$

where the elements in the received noise $\mathbf{N} \in \mathbb{C}^{M_r \times L}$ are independently and identically distributed (i.i.d.) with zero-mean and variance $\sigma^2 > 0$.

With the received signal $\mathrm{vec}(\mathbf{Y})$, the radar receiver uses a filter $\mathbf{w} \in \mathbb{C}^{M_r L \times 1}$ to reduce the interference and noise. Then, the filtered signal is

$$\mathbf{w}^H \mathrm{vec}(\mathbf{Y}) = \mathbf{w}^H[(\mathbf{I}_L \otimes \mathbf{V}_1)\mathbf{s} + (\mathbf{I}_L \otimes \mathbf{V}_2)\mathbf{s} + \mathrm{vec}(\mathbf{N})], \tag{6}$$

where $\mathbf{s} = \mathrm{vec}(\mathbf{S})$. Therefore, the SINR of the radar system is

$$\mathrm{SINR} = \frac{|\mathbf{w}^H(\mathbf{I}_L \otimes \mathbf{V}_1)\mathbf{s}|^2}{|\mathbf{w}^H(\mathbf{I}_L \otimes \mathbf{V}_2)\mathbf{s}|^2 + \sigma^2\|\mathbf{w}\|_2^2}. \tag{7}$$

A. Novel Radar Waveform Constraints

In order to use the efficient nonlinear power amplifier, the constant-modulus constraint is added on $\mathbf{s}$ [7], [14],

$$|\mathbf{s}(n)| = c, \ \forall n \in [1, M_t L], \tag{8}$$

where the constant c is a fixed finite positive number.

Another important constraint is the similarity constraint, which provides an efficient control on the peak sidelobe level and range resolution of the waveform [4]. In particular, by forcing the radar waveform close to a reference waveform $\mathbf{s}_0 \in \mathbb{C}^{M_t L \times 1}$, which has good structure properties. e.g., low modulus variolation, low peak sidelobe level and good range resolution, the soft control on those good structure properties is obtained. The existing similarity constraints are listed as,

$$\|\mathbf{s} - \mathbf{s}_0\|_2 \le \epsilon, \text{in references [4], [6]} \tag{9}$$

$$\|\mathbf{s} - a \cdot \mathbf{s}_0\|_2 \le \epsilon, |a| \le 1, \text{in references [2], [15], [16]} \tag{10}$$

$$\|\mathbf{s} - \mathbf{s}_0\|_\infty \le \epsilon, \text{in references [5], [7], [8]} \tag{11}$$

while the proposed similarity constraint is,

$$\|\mathbf{s} - a \cdot \mathbf{s}_0\|_p \le \epsilon, a \in \mathbb{C}^1, \tag{12}$$

where a is a complex decision variable, $1 \le p \le \infty$[1], the similarity threshold ϵ is a finite nonnegative number. The reasons for the proposed constraint (12) to be a valid similarity constraint are justified as follows.

1) Qualitative Justification: If the reference waveform $\mathbf{s}_0$ has good structure properties, then any phase rotation and nonzero scaling does not change the good structure property of $\mathbf{s}_0$, i.e., $a \cdot \mathbf{s}_0$ with $a \in \mathbb{C}^1$ is also a reference waveform. By decreasing the similarity threshold ϵ in (12), the waveform $\mathbf{s}$ is forced to learn the structure property of $a \cdot \mathbf{s}_0$ and $\mathbf{s}_0$.

2) Quantitative Justification: When $p = 2$, the similarity constraint $\|\mathbf{s} - a \cdot \mathbf{s}_0\|_2^2 \le \epsilon^2$ is the same as

$$\min_a \|\mathbf{s} - a \cdot \mathbf{s}_0\|_2^2 \le \epsilon^2. \tag{13}$$

Since the optimal solution of the convex problem $\min_a \|\mathbf{s} - a \cdot \mathbf{s}_0\|_2^2$ occurs at the unique stationary point $a = \mathbf{s}_0^H\mathbf{s}/\mathbf{s}_0^H\mathbf{s}_0$, the similarity constraint becomes

$$\mathbf{s}^H\mathbf{s} - \frac{|\mathbf{s}_0^H\mathbf{s}|^2}{\mathbf{s}_0^H\mathbf{s}_0} \le \epsilon^2, \tag{14}$$

Since $\mathbf{s} \neq 0$, the constraint (14) can be further transformed to

$$\frac{|\mathbf{s}_0^H\mathbf{s}|^2}{\|\mathbf{s}_0\|_2^2 \cdot \|\mathbf{s}\|_2^2} \ge 1 - \epsilon^2/\|\mathbf{s}\|_2^2 = 1 - \epsilon^2/(M_t L c^2), \tag{15}$$

which is to restrict the normalized correlation between $\mathbf{s}$ and the reference waveform $\mathbf{s}_0$ be sufficiently close to one when $\epsilon \to 0$. This restriction captures the essence of the similarity constraint, i.e., force $\mathbf{s}$ to be similarity with $\mathbf{s}_0$ in terms of global structure.

The waveform $\mathbf{s}_0$ is assumed to be constant-modulus, otherwise the feasible set of (8) and (12) would be a empty set when $\epsilon = 0$. Note that the linear frequency modulated (LFM) waveform is a widely used reference waveform [7].

III. Radar Transceiver Design

The radar waveform design is to maximize the radar SINR subject to the constant-modulus and similarity constraints,

$$\begin{aligned} \max_{\mathbf{s},\mathbf{w},a} \ & \frac{|\mathbf{w}^H(\mathbf{I}_L \otimes \mathbf{V}_1)\mathbf{s}|^2}{|\mathbf{w}^H(\mathbf{I}_L \otimes \mathbf{V}_2)\mathbf{s}|^2 + \sigma^2\|\mathbf{w}\|_2^2} \\ \text{s.t.} \ & |\mathbf{s}(n)| = c, \ \forall n \in [1, M_t L], \\ & \|\mathbf{s} - a \cdot \mathbf{s}_0\|_p \le \epsilon. \end{aligned} \tag{16}$$

The coordinate ascent methodology is use to tackle this difficult nonconvex problem, i.e., alternatively optimizing $\mathbf{w}$ and $\mathbf{s}$.

With fixed $\mathbf{s}$, the SINR can be maximized via $\max_{\mathbf{w}} \mathrm{SINR}$, which is reformulated as

$$\max_{\mathbf{w}} \frac{\mathbf{w}^H\mathbf{\Sigma}_1(\mathbf{s})\mathbf{w}}{\mathbf{w}^H\mathbf{\Sigma}_2(\mathbf{s})\mathbf{w}}, \tag{17}$$

where $\mathbf{\Sigma}_1(\mathbf{s}) = (\mathbf{I}_L \otimes \mathbf{V}_1)\mathbf{s}\mathbf{s}^H(\mathbf{I}_L \otimes \mathbf{V}_1^H)$, and $\mathbf{\Sigma}_2(\mathbf{s}) = (\mathbf{I}_L \otimes \mathbf{V}_2)\mathbf{s}\mathbf{s}^H(\mathbf{I}_L \otimes \mathbf{V}_2^H) + \sigma^2\mathbf{I}$. Since the noise variance

[1] $\|\cdot\|_p$ with $p < 1$ are not mathematic norms.

$\sigma^2 > 0$, the conclusion $\mathbf{\Sigma}_2(\mathbf{s}) \succ 0$ is obtained and the optimal solution of (17) is the normalized eigenvector of $\mathbf{\Sigma}_2(\mathbf{s})^{-1}\mathbf{\Sigma}_1(\mathbf{s})$ corresponding to its largest eigenvalue.

With fixed $\mathbf{w}$, the difficulty of solving $\max_{\mathbf{s}}$ SINR is the nonconvex constant-modulus constraint. We first relax the nonconvex constraint $|\mathbf{s}(n)| = c$ into the convex constraint $|\mathbf{s}(n)| \leq c$, and then retract the constant-modulus of $\mathbf{s}$.

A. Relax the Constant-Modulus Constraint

After relaxing $|\mathbf{s}(n)| = c$ into $|\mathbf{s}(n)| \leq c$, the radar waveform design becomes

$$\begin{aligned} \max_{\mathbf{s},a} \ & \frac{|\mathbf{w}^H(\mathbf{I}_L \otimes \mathbf{V}_1)\mathbf{s}|^2}{|\mathbf{w}^H(\mathbf{I}_L \otimes \mathbf{V}_2)\mathbf{s}|^2 + \sigma^2\|\mathbf{w}\|_2^2} \\ \text{s.t.} & |\mathbf{s}(n)| \leq c, \ \forall n \in [1, M_t L], \\ & \|\mathbf{s} - a \cdot \mathbf{s}_0\|_p \leq \epsilon, \end{aligned} \tag{18}$$

its the objective function is still a nonconvex function of $\mathbf{s}$. However, with a square-root transformation, the problem (18) is the same as

$$\begin{aligned} \max_{\mathbf{s},a} \ & \frac{|\mathbf{w}^H(\mathbf{I}_L \otimes \mathbf{V}_1)\mathbf{s}|}{\sqrt{|\mathbf{w}^H(\mathbf{I}_L \otimes \mathbf{V}_2)\mathbf{s}|^2 + \sigma^2\|\mathbf{w}\|_2^2}} \\ \text{s.t.} & |\mathbf{s}(n)| \leq c, \ \forall n \in [1, M_t L], \\ & \|\mathbf{s} - a \cdot \mathbf{s}_0\|_p \leq \epsilon, \end{aligned} \tag{19}$$

Note that if $(\mathbf{s}, a)$ is an optimal solution of problem (19), then $(\mathbf{s} \cdot e^{j\theta}, a \cdot e^{j\theta})$ with any $\theta \in [0, 2\pi]$ is also an optimal solution of problem (19). Therefore, the problem (19) is the same as

$$\begin{aligned} \max_{\mathbf{s},a} \ & \frac{\mathrm{Re}(\mathbf{w}^H(\mathbf{I}_L \otimes \mathbf{V}_1)\mathbf{s})}{\sqrt{|\mathbf{w}^H(\mathbf{I}_L \otimes \mathbf{V}_2)\mathbf{s}|^2 + \sigma^2\|\mathbf{w}\|_2^2}} \\ \text{s.t.} \ & \mathrm{Im}(\mathbf{w}^H(\mathbf{I}_L \otimes \mathbf{V}_1)\mathbf{s}) = 0 \\ & |\mathbf{s}(n)| \leq c, \ \forall n \in [1, M_t L], \\ & \|\mathbf{s} - a \cdot \mathbf{s}_0\|_p \leq \epsilon. \end{aligned} \tag{20}$$

Although the problem (20) is still a nonconvex problem, its special objective function and convex feasible set allow it be solved optimally in [17]. Since the radar receiver $\mathbf{w} \neq 0$ and noise variance $\sigma^2 > 0$, the objective function of problem (20) is a ratio of a concave (linear) function over a positive convex function. Furthermore, the feasible set of problem (20) is a convex compact set on $(\mathbf{s}, a)$. Therefore, [17] reveals that the optimal solution of problem (20) is obtained by solving a series of second-order cone programming (SOCP) problems (21) through Algorithm 1.

$$\begin{aligned} \max_{\mathbf{s},a} \ & \mathrm{Re}(\mathbf{w}^H(\mathbf{I}_L \otimes \mathbf{V}_1)\mathbf{s}) \\ & - q\sqrt{|\mathbf{w}^H(\mathbf{I}_L \otimes \mathbf{V}_2)\mathbf{s}|^2 + \sigma^2\|\mathbf{w}\|_2^2} \\ \text{s.t.} \ & \mathrm{Im}(\mathbf{w}^H(\mathbf{I}_L \otimes \mathbf{V}_1)\mathbf{s}) = 0, \\ & |\mathbf{s}(n)| \leq c, \ \forall n \in [1, M_t L], \\ & \|\mathbf{s} - a \cdot \mathbf{s}_0\|_p \leq \epsilon. \end{aligned} \tag{21}$$

The monotonic convergence property and optimality of Algorithm 1 are proved in [17].

With the optimized $\mathbf{w}$ and $\mathbf{s}$, an iterative algorithm to obtain the radar transceiver is proposed in Algorithm 2. Since the proposed Algorithm 2 is to alternatively maximize the SINR, and the optimal solutions for $\mathbf{s}$ and $\mathbf{w}$ are obtained, the optimized SINR has to be monotonically nondecreasing. Together with the fact that the SINR is upper bounded by a finite value, the convergence of the Algorithm 2 is guaranteed.

Denote the converged solution in Algorithm 2 as $(\mathbf{s}_i, \mathbf{w}^\star)$, and let the converged SINR be $\gamma^\star$.

Algorithm 1 Relaxed Radar Transmitter in (18).

1: **initialization:** set $n = 0$.
2: **repeat**
3: Set $n = n + 1$, update $q = \frac{|\mathbf{w}^H(\mathbf{I}_L \otimes \mathbf{V}_1)\mathbf{s}|}{\sqrt{|\mathbf{w}^H(\mathbf{I}_L \otimes \mathbf{V}_2)\mathbf{s}|^2 + \sigma^2\|\mathbf{w}\|_2^2}}$ with the latest feasible $(\mathbf{w}, \mathbf{s})$, solve problem (21) and denote its objective value as $J[n]$.
4: **until** $J[n] \leq \epsilon_1$.

Algorithm 2 Radar Transceiver Design.

1: **initialization:** set $\mathbf{s} = \mathbf{s}_0, i = 0$.
2: **repeat**
3: Find the optimal receiver $\mathbf{w}$ in problem (17)
4: Set $i = i + 1$, use Algorithm 1 to find the optimal transmitters and denote the obtained SINR as $\mathrm{SINR}[i]$.
5: **until** $i \geq 2$ and $(\mathrm{SINR}[i] - \mathrm{SINR}[i-1])/\mathrm{SINR}[i] \leq \epsilon_2$, or $i >= i_{max}$.

B. Retract the Constant-Modulus

After Algorithm 2, $\mathbf{s}_i$ learns the global structure property of $\mathbf{s}_0$ with the similarity constraint. It is time to recover the constant-modulus in the local area with guaranteed SINR performance, i.e., $\frac{|\mathbf{w}^H(\mathbf{I}_L \otimes \mathbf{V}_1)\mathbf{s}|}{\sqrt{|\mathbf{w}^H(\mathbf{I}_L \otimes \mathbf{V}_2)\mathbf{s}|^2 + \sigma^2\|\mathbf{w}\|_2^2}} \geq \sqrt{\gamma^\star}$ is needed for the recovering process. Note that the following convex constraint is sufficient to guarantee the SINR performance,

$$\sqrt{|\underbrace{(\mathbf{w}^\star)^H(\mathbf{I}_L \otimes \mathbf{V}_2)}_{\mathbf{v}_2^H}\mathbf{s}|^2 + \sigma^2} \leq \frac{1}{\sqrt{\gamma^\star}}\mathrm{Re}(\underbrace{(\mathbf{w}^\star)^H(\mathbf{I}_L \otimes \mathbf{V}_1)}_{\mathbf{v}_1^H}\mathbf{s}), \tag{22}$$

where $\mathbf{s} = \mathbf{s}_i$ satisfies the constraint.

Although the retract operation in [12] is good for geometric illustration, a simper retract operation is proposed in the following SOCP problem,

$$\begin{aligned} \max_{\mathbf{s}} \ & \mathrm{Re}(\mathbf{s}_i^H\mathbf{s}) \\ \text{s.t.} \ & \mathbf{s} \in \underbrace{\{\mathbf{s} | \sqrt{|(\mathbf{v}_2^H\mathbf{s}|^2 + \sigma^2} \leq \frac{1}{\sqrt{\gamma^\star}}\mathrm{Re}((\mathbf{v}_1^H\mathbf{s})\}}_{\mathcal{S}_{\gamma^\star}}, \\ & \mathbf{s} \in \underbrace{\{\mathbf{s} | |\mathbf{s}(n)| \leq c, \ \forall n \in [1, M_t L]\}}_{\mathcal{S}_b}, \end{aligned} \tag{23}$$

where the optimal solution is denoted as $\mathbf{s}_{i+1}$. Since $\mathbf{s}_i$ is a feasible solution of the problem (23), we obtain

$$\mathrm{Re}(\mathbf{s}_i^H\mathbf{s}_i) = \|\mathbf{s}_i\|_2^2 \leq \mathrm{Re}(\mathbf{s}_i^H\mathbf{s}_{i+1}) = \mathrm{Re}(\mathbf{s}_i^H(\mathbf{s}_i + \boldsymbol{\xi})), \tag{24}$$

Algorithm 3 Retract operation.

1: **repeat**
2: Solve the convex problem (23), denote the optimal solution as $\mathbf{s}_{i+1}$.
3: If $\|\mathbf{s}_{i+1}\|_2^2 - \|\mathbf{s}_i\|_2^2 \le \epsilon_3$ and $\|\mathbf{s}_{i+1}\|_2^2 < M_tL(c^2-\epsilon_4^2)$, find the index $k = \arg\min\{|\mathbf{s}_{i+1}(k)|\}_{k=1}^{M_tL}$, solve the convex problem (26), denote the optimal solution as $\bar{s}$. Update $\mathbf{s}_{i+1}(k) = \bar{s}$.
4: Update $i = i+1$.
5: **until** $c - \min\{|\mathbf{s}_i(n)|\}_{n=1}^{M_tL} \le \epsilon_4$

which implies $\mathrm{Re}(\mathbf{s}_i^H\boldsymbol{\xi}) \ge 0$. This leads to

$$\|\mathbf{s}_i\|_2^2 \le \|\mathbf{s}_{i+1}\|_2^2 = \|\mathbf{s}_i+\boldsymbol{\xi}\|_2^2 = \|\mathbf{s}_i\|_2^2 + \|\boldsymbol{\xi}\|_2^2 + 2\mathrm{Re}(\mathbf{s}_i^H\boldsymbol{\xi}). \tag{25}$$

Therefore, the norm of the waveform is monotonically increased in Algorithm 3. the monotonic property $\|\mathbf{s}_i\|_2^2 \le \|\mathbf{s}_{i+1}\|_2^2$ and the boundary condition $\|\mathbf{s}_{i+1}\|_2^2 \le M_tLc^2$ guarantee that the sequence $\{\|\mathbf{s}_i\|_2^2\}_{i=1}^{\infty}$ is to be converged. However, the converged solution is not guaranteed to be a constant-modulus solution with $\|\mathbf{s}_\infty\|_2^2 = M_tLc^2$.

If $\|\mathbf{s}_i\|_2^2 = \|\mathbf{s}_{i+1}\|_2^2 < M_tLc^2$ in (25), the following convex program is used to update $\mathbf{s}_{i+1}(k)$, where k is the index with minimal modulus $|\mathbf{s}_{i+1}(k)|$,

$$\begin{aligned}
&\max_{s}\ \mathrm{Re}(-\mathbf{s}_{i+1}^H(k)\cdot s)\\
&\text{s.t. } \sqrt{|\mathbf{v}_2^H(k)s + \sum_{n=1,n\neq k}^{M_tL}\mathbf{v}_2^H(n)\mathbf{s}_{i+1}(n))|^2+\sigma^2}\\
&\le \frac{1}{\sqrt{\gamma^\star}}\mathrm{Re}(\mathbf{v}_1^H(k)s + \sum_{n=1,n\neq k}^{M_tL}\mathbf{v}_1^H(n)\mathbf{s}_{i+1}(n))),\\
&|s| \le c,
\end{aligned} \tag{26}$$

where the optimal solution is denoted as $\bar{s}$. The $\mathbf{s}_{i+1}$ is updated as $\mathbf{s}_{i+1}(k) = \bar{s}$, then the strict inequality $\|\mathbf{s}_i\|_2^2 < \|\mathbf{s}_{i+1}\|_2^2$ is expected. The retract operation is described in Algorithm 3, its property is summarized as follows.

Theorem 1. *In Algorithm 3, the converged solution $\mathbf{s}_{i+i_3}$ is a constant-modulus solution, and the iteration number $i_3 \in [1, M_tL]$.*

Proof. The problem (23) is the same as

$$\begin{aligned}
&\max_{\mathbf{s}}\ \mathrm{Re}(\mathbf{s}_i^H\mathbf{s})\\
&\text{s.t. } \mathbf{s} \in \mathcal{S}_b \cap \mathcal{S}_{\gamma^\star}.
\end{aligned} \tag{27}$$

The SOCP constraint in (23) reveals that the convex set $\mathcal{S}_{\gamma^\star}$ is unbounded with a hyperbolic boundary. We can recover the two-branch hyperbolic set from the one-branch hyperbolic set $\mathcal{S}_{\gamma^\star}$ as follows,

$$\text{one-branch hyperbolic: } \sqrt{|\mathbf{v}_2^H\mathbf{s}|^2+\sigma^2} \le \frac{1}{\sqrt{\gamma^\star}}\mathrm{Re}(\mathbf{v}_1^H\mathbf{s}), \tag{28}$$

$$\text{two-branch hyperbolic: } \sqrt{|\mathbf{v}_2^H\mathbf{s}|^2+\sigma^2} \le \frac{1}{\sqrt{\gamma^\star}}|\mathbf{v}_1^H\mathbf{s}|. \tag{29}$$

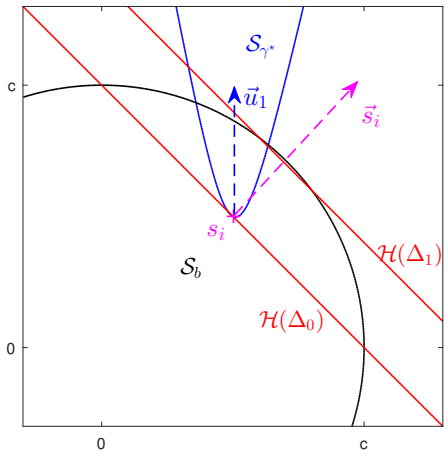

Fig. 1. $\vec{\mathbf{s}}_i$: normal vector of the moving hyperplane $\mathcal{H}(\Delta)$. $\vec{\mathbf{u}}_1$: normal vector of the directrix for the hyperbolic set $\mathcal{S}_{\gamma^\star}$.

With a square transformation, (29) can be reformulated as

$$\mathbf{s}^H\underbrace{\left[\frac{\mathbf{v}_1\mathbf{v}_1^H}{\gamma^\star\sigma^2} - \frac{\mathbf{v}_2\mathbf{v}_2^H}{\sigma^2}\right]}_{\mathbf{A}}\mathbf{s} \ge 1. \tag{30}$$

Since $\mathbf{A} = \mathbf{A}^H$, with a eigenvalue decomposition, we have

$$\mathbf{A} = [\mathbf{u}_1, \mathbf{u}_2]\cdot\mathrm{Diag}([\lambda_1,\lambda_2])\cdot[\mathbf{u}_1,\mathbf{u}_2]^H. \tag{31}$$

Therefore, the equation (30) becomes

$$-\lambda_2|\mathbf{u}_2^H\mathbf{s}|^2 + 1 \le \lambda_1|\mathbf{u}_1^H\mathbf{s}|^2. \tag{32}$$

For radar application, the received target signal power is not zero, i.e., $\mathbf{v}_1 \neq 0$, $\gamma^\star < 1$ when $\mathbf{v}_1 = \mathbf{v}_2$. Therefore, the properties of the eigenvalues are $\lambda_1 > 0, \lambda_2 \le 0$. Since $\mathbf{u}_1 e^{j\theta}$ with any $\theta \in [0, 2\pi]$ are the eigenvectors of $\mathbf{A}$ associated with λ_1, we can choose $\mathbf{u}_1$ such that $\mathrm{Re}(\mathbf{u}_1^H\mathbf{s}) = |\mathbf{u}_1^H\mathbf{s}|$. Then, we can recover the one-branch hyperbolic case as

$$\sqrt{-\lambda_2|\mathbf{u}_2^H\mathbf{s}|^2+1} \le \sqrt{\lambda_1}\mathrm{Re}(\mathbf{u}_1^H\mathbf{s}), \tag{33}$$

which is the same constraint as (28). Since $\mathbf{s}_i$ satisfies the constraint in (28), $\mathbf{s}_i$ also satisfies the constraint in (33). Then, we have

$$0 < \mathrm{Re}(\mathbf{u}_1^H\mathbf{s}_i), \tag{34}$$

which means that the angle between $\mathbf{u}_1$ and $\mathbf{s}_i$ is smaller than 90^o.

For better geometric illustration, the problems (23) and (27) can be transformed to

$$\begin{aligned}
&\max_{\mathbf{s},\Delta}\ \Delta\\
&\text{s.t. } \mathbf{s} \in \mathcal{S}_b \cap \mathcal{S}_{\gamma^\star}, \overbrace{\mathrm{Re}(\mathbf{s}_i^H\mathbf{s}) = \Delta}^{\mathcal{H}(\Delta)},
\end{aligned} \tag{35}$$

where $\mathcal{H}(\Delta)$ can be interpreted as a moving hyperplane.

Since the normal of the moving hyperplane $\mathcal{H}(\Delta)$ is $\mathbf{s}_i$ and $\mathbf{u}_1$ is the normal of the directrix for the hyperbolic set $\mathcal{S}_{\gamma^\star}$,

the conclusion $0 < \mathrm{Re}(\mathbf{u}_1^H \mathbf{s}_i)$ means that the angle between the normal of the directrix for the hyperbolic set $\mathcal{S}_{\gamma^\star}$ and the normal of the moving hyperplane $\mathcal{H}(\Delta)$ is smaller than 90^o, i.e., the hyperplane $\mathcal{H}(\Delta)$ is moving towards the unbounded side of $\mathcal{S}_{\gamma^\star}$. This geometric phenomenon is illustrated in Fig. 1.

The optimization problem (26) can be implemented by increasing Δ from $\|\mathbf{s}_i\|_2^2$, which is generated from the feasible solution $\mathbf{s} = \mathbf{s}_i$, unless the hyperplane cannot move anymore when it stopped by the extreme point of $\mathcal{S}_b \cap \mathcal{S}_{\gamma^\star}$, i.e., the optimal hyperplane $\mathcal{H}(\Delta^\star)$ becomes a supporting hyperplane of $\mathcal{S}_b \cap \mathcal{S}_{\gamma^\star}$. Since the angle between the normal of the directrix for the hyperbolic set $\mathcal{S}_{\gamma^\star}$ and the normal of the moving hyperplane $\mathcal{H}(\Delta)$ is smaller than 90^o, the movement of the hyperplane will not be stopped by the unbounded set $\mathcal{S}_{\gamma^\star}$ alone even when $\Delta \to +\infty$. However, since $\mathcal{S}_b$ is a bounded set, the movement of the hyperplane can be stopped by the extreme point of $\mathcal{S}_b$. Therefore, the optimal solution of problem (27) only happens for the following two cases.

Case A: $\mathcal{H}(\Delta^\star)$ touches the boundaries of $\mathcal{S}_b$, i.e., $|\mathbf{s}_{i+1}(n)| = c,\ \forall n \in [1, M_t L]$ or $\|\mathbf{s}_{i+1}\|_2^2 = M_t L c^2$.

Case B: $\mathcal{H}(\Delta^\star)$ is a supporting hyperplane of $\mathcal{S}_b \cap \mathcal{S}_{\gamma^\star}$. In particular, some subspaces of $\mathcal{H}(\Delta^\star)$ with lines $\{\mathcal{H}_n\}$ touches the boundaries of the sets $\{|\mathbf{s}(n)| \le c\}$, while other subspaces of $\mathcal{H}(\Delta^\star)$ with lines $\{\mathcal{H}_k\}$ are supporting hyperplanes of the subspace of $\mathcal{S}_{\gamma^\star}$.

After the above geometric analysis, we can estimate the lower bound of $\|\mathbf{s}_{i+1}\|_2^2$ as follows. With the optimal solution $\mathbf{s}_{i+1}$ from the problem (23), there are only two cases:

1) $\|\mathbf{s}_i\|_2^2 < \|\mathbf{s}_{i+1}\|_2^2$, i.e., at least one point $\mathbf{s}_{i+1}(k)$ in the k-th subspace can move away from $\mathbf{s}_i(k)$. In fact, with other points $\{\mathbf{s}(n)\}_{n=1,n\neq k}^{M_t L}$ being fixed, the point $\mathbf{s}_{i+1}(k)$ can touches the boundary of $|\mathbf{s}(k)| = c$. Then, we have $\|\mathbf{s}_{i+1}\|_2^2 \ge 1 \cdot c^2$
2) $\|\mathbf{s}_i\|_2^2 = \|\mathbf{s}_{i+1}\|_2^2 < M_t L c^2$, i.e., no point $\mathbf{s}_{i+1}(k)$ in the k-th subspace can move away from $\mathbf{s}_i(k)$. This phenomenon is illustrated in Fig. 2, where $|\mathbf{s}_{i+1}(k)| < c$ and the index $k = \arg\min\{|\mathbf{s}_{i+1}(k)|\}_{k=1}^{M_t L}$. After reversing the normal direction of the hyperplane $\mathcal{H}_k$ in the subspace as we changed the objective function in problem (26), its optimal solution $\bar{s}$ occurs at the boundary of the set $|s| \le c$, i.e., $|\bar{s}| = c$. With the update $\mathbf{s}_{i+1}(k) = \bar{s}$, we have $\|\mathbf{s}_{i+1}\|_2^2 \ge 1 \cdot c^2$.

Therefore, from $\mathbf{s}_i$ to $\mathbf{s}_{i+1}$, we have the lower bound $\|\mathbf{s}_{i+1}\|_2^2 \ge 1 \cdot c^2$. The same analysis can be generalized to $\|\mathbf{s}_{i+i_3}\|_2^2 \ge i_3 \cdot c^2$. Since the upper bound is $\|\mathbf{s}\|_2^2 \le M_t L c^2$, the iteration number $i_3 \le M_t L$. At the worst case, $\mathbf{s}_{i+M_t L}$ is a constant-modulus solution. □

C. Relax-and-Retract Algorithm & Its Properties

The proposed relax-and-retract algorithm is to execute Algorithm 2 first, if the numeric constant-modulus condition is not satisfied[2], i.e., $c - \min\{|\mathbf{s}_i(n)|\}_{n=1}^{M_t L} > \epsilon_4$ with ϵ_4 being the desired numeric precision, then the Algorithm 3 is implemented last. The properties of the proposed relax-and-retract algorithm are summarized as follows.

[2]The numeric error is unavoidable.

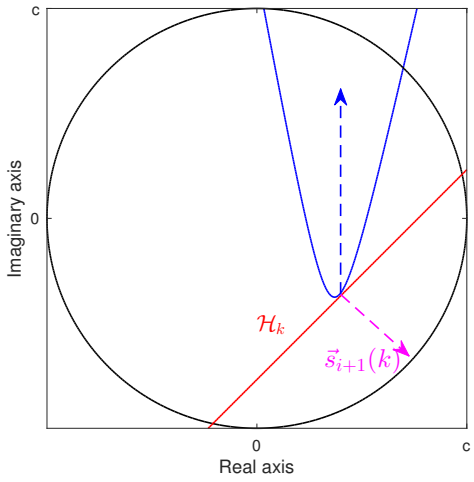

Fig. 2. Illustration for the case $\|\mathbf{s}_i\|_2^2 = \|\mathbf{s}_{i+1}\|_2^2 < M_t L c^2$ in the k-th subspace.

1) Full range similarity control: Although all convex subproblems of Algorithms 2 and 3 are solved by the interior point method, the solutions can also be obtained by the gradient method, i.e., the final waveform $\mathbf{s}$ is a continuous deformation of $\mathbf{s}_0$ as the parameter ϵ increased from zero to infinity. That is to say the full range similarity control is achieved by the proposed relax-and-retract algorithm.

2) Impact of p : It can be shown that $\|\mathbf{s}\|_{p1} \ge \|\mathbf{s}\|_{p2}$ if $p1 < p2$ and $p1, p2 \in [1, \infty]$. Therefore, with the same ϵ, the constraint $\|\mathbf{s} - a \cdot \mathbf{s}_0\|_p \le \epsilon$ with smaller p leads to more stringent requirement on similarity control.

3) 1-norm as a constant-modulus-inducing norm: The 1-norm, $\|\mathbf{s} - a \cdot \mathbf{s}_0\|_1 \le \epsilon$, is a well-known sparsity-inducing norm, i.e., forcing the elements of $\mathbf{s} - a \cdot \mathbf{s}_0$ being zeros with a relative small ϵ, instead of closing to zero for large p-norms. Therefore, in a large region $\epsilon \in [0, r_{p1}]$, the relaxation solution of Algorithm 2, without retract operation, will be constant-modulus solution. Therefore, 1-norm similarity constraint with a constant-modulus $\mathbf{s}_0$ is a constant-modulus-inducing norm.

4) Computational complexity: Since all subproblems of the proposed algorithm are SOCP problems, the complexity order is $\mathcal{O}((i_1 i_2 + i_3)(M_t L)^{3.5})$ [18], where i_1, i_2, i_3 are the average iteration number of Algorithms 1 to 3, respectively. For the ∞-norm, the complexity order of the proposed method is comparable to that of $\mathcal{O}((i_{out} i_{in})(M_t L)^{3.5})$ in the SQR method [8] and smaller than that of $\mathcal{O}((i_{out} i_{in})(M_t L)^{4.5})$ in SDR method [7]. In fact, the dimension of the $M_t L$ quadratic constraints [8] in is $M_t L$, while that of the proposed method is one. Furthermore, the extra $2M_t L$ dense linear constraints also make the computational complexity of the SQR method would be larger than the proposed method.

IV. Simulation and Discussion

In the MIMO radar system, the antenna numbers are $M_t = 4, M_r = 8$, the waveform length is $L = 16$, and the antenna arrays are half-wavelength uniform linear arrays. The target angle with respect to the array is 15^o, the point scatters

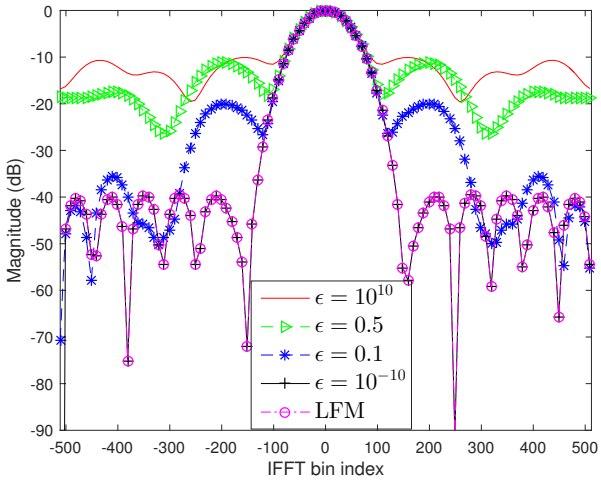

(a) Similarity control

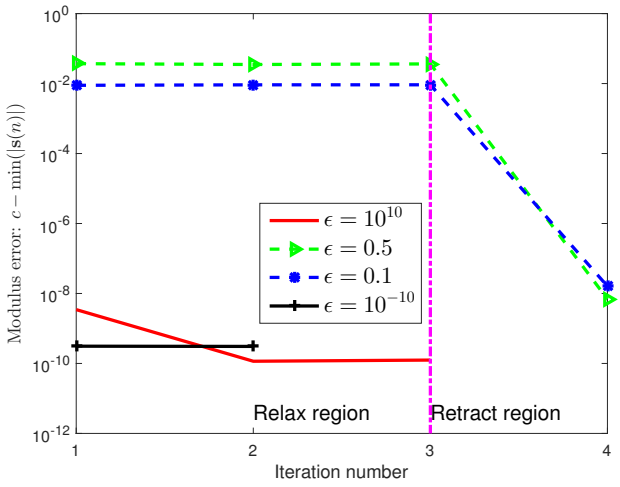

(b) Constant-modulus checking

Fig. 3. 2-norm similarity control under different ϵ.

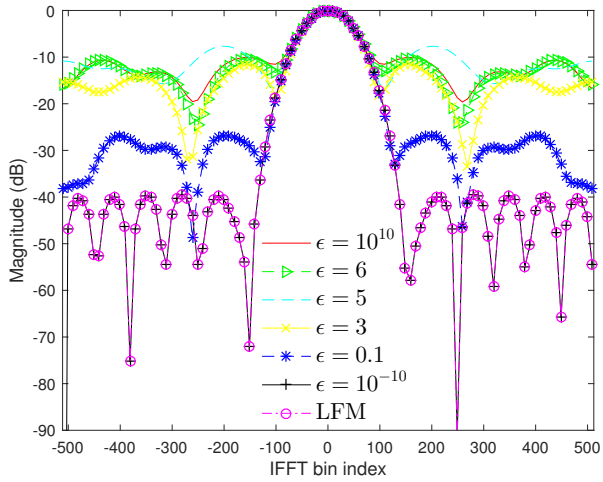

(a) Similarity control

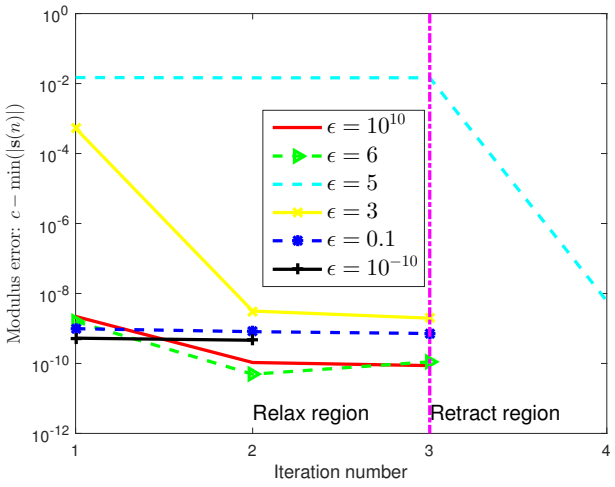

(b) Constant-modulus checking

Fig. 4. 1-norm similarity control under different ϵ.

are estimated at angles $-50^o, -10^o$ and 40^o. The reflection coefficients of the clutters and the target are estimated as $\{\beta_k^c = \sqrt{10}\}$ and $\beta_1 = \sqrt{10}$, respectively. The Doppler shifts of the targets and clutters are set to be zero. The noise variance of the radar receivers is set as $\sigma^2 = 1$. The reference waveform $\mathbf{s}_0$ is the LFM waveform, and $c = 1/\sqrt{M_t L}$. The terminate parameters are $\epsilon_1 = 10^{-2}, \epsilon_2 = 10^{-3}, \epsilon_3 = \epsilon_4 = 10^{-6}, i_{max} = 3$ unless noted otherwise. All optimization problems are solved on a laptop PC with 3.6 GHz CPU and 16GB RAM, using the solver CVX [19].

A. Similarity Control and Constant-Modulus Checking for Different p-Norms

The performance of 2-norm similarity constraint is illustrated in Fig. 3. Fig. 3(a) shows that $\mathbf{s}$ is sufficiently close to LFM $\mathbf{s}_0$ with $\epsilon = 10^{-10}$, while $\mathbf{s}$ is far away from $\mathbf{s}_0$ with $\epsilon = 10^{10}$. The pulse compression profile in Fig. 3(a) shows that the sidelopes increase with ϵ. Therefore, with a proper ϵ, the desired sidelope property can be achieved. Fig. 3(b) shows that the constant-modulus requirements are satisfied, up to a numeric error 10^{-8}.

Fig. 4 describes the performance of 1-norm similarity constraint. The pulse compression profile in Fig. 4(a) shows that the sidelopes increase with ϵ. Fig. 4(b) shows that the constant-modulus requirements are satisfied. In particular, with a large region $\epsilon \in [0, 3]$, the constant-modulus requirements are satisfied without the retract operation, which validates the constant-modulus-inducing norm conclusion in Section III-C3.

Fig. 5 reveals the performance of different p-norm similarity constraint with fixed $\epsilon = 0.1$. The pulse compression profile in Fig. 5(a) shows that the sidelopes increase with p, which validates the conclusion in Section III-C2. Fig. 5(b) shows that the constant-modulus requirements are satisfied for all p-norms.

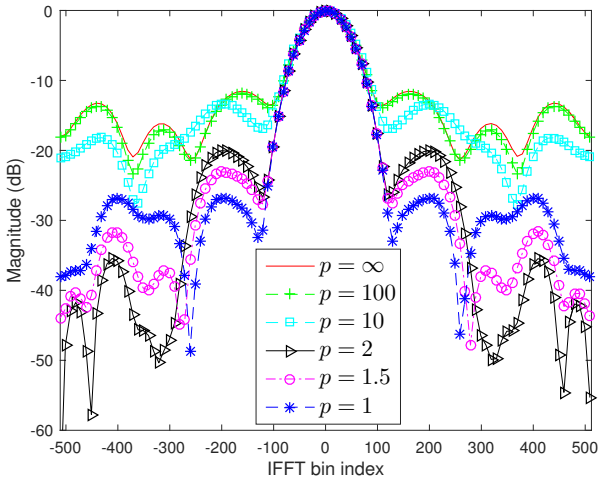

(a) Similarity control

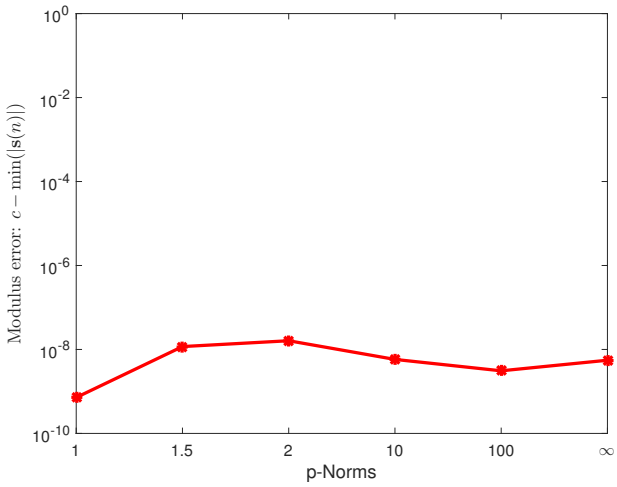

(b) Constant-modulus checking

Fig. 5. Different p-norm similarity control with $\epsilon = 0.1$.

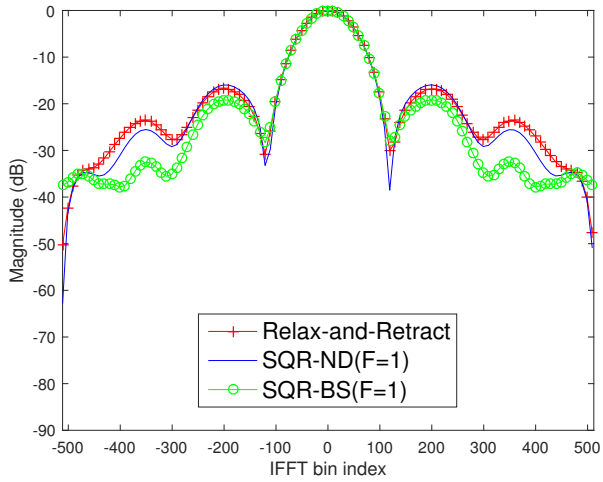

(a) Similarity control

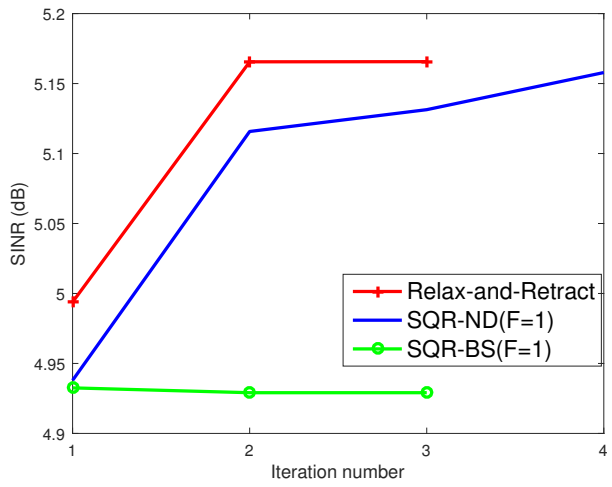

(b) SINR performance

Fig. 6. Similarity control and SINR performance under different methods with ∞-norm.

B. Comparison With SQR Method for ∞-Norm

In order to fairly compared with the SQR methods [8], the terminate parameters for SQR and the proposed method are set as $\epsilon_2 = 10^{-2}, i_{max} = 20$. Since the formulations of the similarity constraint for the two methods are different, the values ϵ for the two methods are different. To get similar similarity control, $\epsilon = 0.2$ is set for the SQR method, while $\epsilon = 0.0225$ is set for the proposed method. Fig. 6 shows that the SQR methods and the proposed relax-and-retract method achieve similar similarity control and SINR performance. However, the computational time performance in Fig. 7 shows that the computational time of the relax-and-retract method is smaller than that of the SQR methods, which validates the computational analysis in Section III-C4.

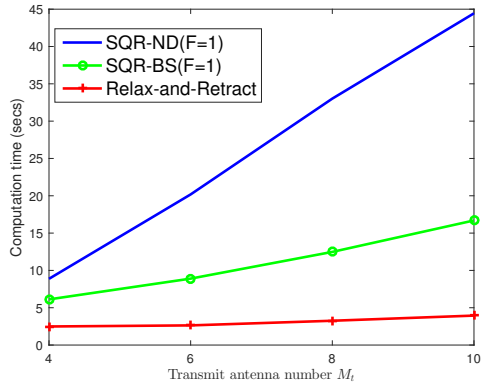

Fig. 7. Computational times under different methods with ∞-norm.

V. Conclusion

In this study, the radar waveform design under joint constant-modulus and any p-norm ($1 \leq p \leq \infty$) similarity constraint is tackled by the proposed relax-and-retract algo-

rithm. Extensive simulation results show that full range similarity control and constant-modulus constraints are satisfied under different p-norms. For the special case with 1-norm, it is firstly found to be a constant-modulus-inducing norm. For the special case with ∞-norm, the proposed relax-and-retract method has less computational time than the SDR and SQR methods.

VI. Acknowledgment

We would like to thank Prof. Jiangzhou Wang in University of Kent for his encouragement and correcting typos in a draft version (not this version). We would like to thank Prof. Lei Huang in Shenzhen University for correcting typos in a draft version (not this version).

References

[1] S. Feng and S. Haykin, "Cognitive risk control for transmit-waveform selection in vehicular radar systems," *IEEE Transactions on Vehicular Technology*, vol. 67, no. 10, pp. 9542–9556, 2018.

[2] Z. Cheng, B. Liao, Z. He, J. Li, and J. Xie, "Joint design of the transmit and receive beamforming in MIMO radar systems," *IEEE Transactions on Vehicular Technology*, vol. 68, no. 8, pp. 7919–7930, 2019.

[3] X. He and L. Huang, "Joint MIMO communication and MIMO radar under different practical waveform constraints," *IEEE Transactions on Vehicular Technology*, vol. 69, no. 12, pp. 16 342–16 347, 2020.

[4] J. Li, J. R. Guerci, and L. Xu, "Signal waveform's optimal-under-restriction design for active sensing," *IEEE Signal Processing Letters*, vol. 13, no. 9, pp. 565–568, 2006.

[5] A. De Maio, S. De Nicola, Y. Huang, Z. Luo, and S. Zhang, "Design of phase codes for radar performance optimization with a similarity constraint," *IEEE Transactions on Signal Processing*, vol. 57, no. 2, pp. 610–621, 2009.

[6] A. De Maio, S. De Nicola, Y. Huang, S. Zhang, and A. Farina, "Code design to optimize radar detection performance under accuracy and similarity constraints," *IEEE Transactions on Signal Processing*, vol. 56, no. 11, pp. 5618–5629, 2008.

[7] G. Cui, H. Li, and M. Rangaswamy, "MIMO radar waveform design with constant modulus and similarity constraints," *IEEE Transactions on Signal Processing*, vol. 62, no. 2, pp. 343–353, 2014.

[8] O. Aldayel, V. Monga, and M. Rangaswamy, "Successive qcqp refinement for MIMO radar waveform design under practical constraints," *IEEE Transactions on Signal Processing*, vol. 64, no. 14, pp. 3760–3774, 2016.

[9] X. Yu, K. Alhujaili, G. Cui, and V. Monga, "MIMO radar waveform design in the presence of multiple targets and practical constraints," *IEEE Transactions on Signal Processing*, vol. 68, pp. 1974–1989, 2020.

[10] L. Wu, P. Babu, and D. P. Palomar, "Transmit waveform/receive filter design for MIMO radar with multiple waveform constraints," *IEEE Transactions on Signal Processing*, vol. 66, no. 6, pp. 1526–1540, 2018.

[11] X. Yu, G. Cui, J. Yang, and L. Kong, "MIMO radar transmit-receive design for moving target detection in signal-dependent clutter," *IEEE Transactions on Vehicular Technology*, vol. 69, no. 1, pp. 522–536, 2020.

[12] X. He, L. Huang, and J. Wang, "Novel relax-and-retract algorithm for intelligent reflecting surface design," *IEEE Transactions on Vehicular Technology*, vol. 70, no. 2, pp. 1995–2000, 2021.

[13] B. Li and A. P. Petropulu, "Joint transmit designs for coexistence of MIMO wireless communications and sparse sensing radars in clutter," *IEEE Transactions on Aerospace and Electronic Systems*, vol. 53, no. 6, pp. 2846–2864, Dec 2017.

[14] Z. Cheng, Z. He, S. Zhang, and J. Li, "Constant modulus waveform design for MIMO radar transmit beampattern," *IEEE Transactions on Signal Processing*, vol. 65, no. 18, pp. 4912–4923, 2017.

[15] Z. Cheng, B. Liao, Z. He, Y. Li, and J. Li, "Spectrally compatible waveform design for MIMO radar in the presence of multiple targets," *IEEE Transactions on Signal Processing*, vol. 66, no. 13, pp. 3543–3555, 2018.

[16] A. Aubry, V. Carotenuto, and A. D. Maio, "Forcing multiple spectral compatibility constraints in radar waveforms," *IEEE Signal Processing Letters*, vol. 23, no. 4, pp. 483–487, 2016.

[17] W. Dinkelbach, "On nonlinear fractional programming," *Management Science*, vol. 13, no. 7, pp. 492–498, 1967.

[18] Z.-Q. Luo and W. Yu, "An introduction to convex optimization for communications and signal processing," *IEEE Journal on Selected Areas in Communications*, vol. 24, no. 8, pp. 1426–1438, 2006.

[19] M. Grant and S. Boyd, "CVX: Matlab software for disciplined convex programming, version 2.1," http://cvxr.com/cvx, Mar. 2014.